Treatments

Pregnant rats were injected with 60 mg/kg of ENU (Sigma, St. Louis, MO) or an equivalent volume of buffer (2 mM sodium citrate buffer) alone intraperitoneally on Day 13 of gestation, and dams were euthanized and fetuses were collected at 3, 6, 12, 24, and 48 hr after the treatment, respectively. Fetal telencephalon was excised from a fetus and subjected to the cell cycle and microarray analyses.

Cell Cycle Analysis by Laser Scanning Cytometer

Two fetal telencephalons from a dam were pooled and cells were isolated by mechanical trituration. After being washed with PBS, cells were smeared onto a slide glass by CytoFuge2 (StatSpin, Norwood, MA) and fixed in 70% ethanol at 4°C. Cells were treated with RNase A (Sigma) and stained with propidium iodide (Sigma). Cell cycle phase analysis was carried out using a laser scanning cytometer (Olympus, Tokyo, Japan). Ten thousand cells were examined in each sample. Using the WinCyte analysis software (Olympus), doublets and debris were discarded and then percentages of cells in the various phases of the cell cycle were calculated.

Microarray Analysis

Four to six fetal telencephalons from a dam were pooled and total RNA was isolated with RNeasy Protect Kit (Qiagen, Tokyo, Japan) according to the manufacturer's instructions. Microarray analysis was carried out according to the Affymetrix Expression Analysis Technical Manual (Affymetrix, Santa Clara, CA). Briefly, the second strand cDNA was prepared from total RNA using the SuperScript Double Strand cDNA Synthesis kit (Invitrogen, Carlsbad, CA) with T7-$(dT)_{24}$ primer (primer sequence: 5′-GGC CAG TGA ATT GTA ATA CGA CTC ACT ATA GGG AGG CGG-$(dT)_{24}$-3′, Amersham Biosciences, Piscataway, NJ). Then, biotin-labeled cRNA was synthesized from the double-stranded cDNA using the Enzo High Yield RNA Transcription Labeling Kit (Enzo Life Sciences, Farmingdale, NY). The hybridization solution was prepared with GeneChip Eukaryotic Hybridization Control Kit (Affymetrix), and hybridized to the Affymetrix Rat Expression Array U34A for 16 hr at 45°C in GeneChip Hybridization Oven 640 (Affymetrix). The chips were then washed and stained using the Fluidics Station (Affymetrix), and scanned with GeneArray Scanner (Hewlett Packard, Palo Alto, CA). Microarray analyses were carried out twice in each time point using total RNA samples from independent pairs of ENU-treated and control dams.

Microarray Data Analysis

The microarray imaging data were analyzed using the MicroarraySuite (Affymetrix). After hybridization intensity data were captured, intensity values of each probe were automatically calculated. Data were compared between the ENU-treated and control groups. Before comparing any two measurements, scaling (target signal value = 500) and global normalizing procedure were carried out. The fold change was derived by the ratio of average differences from one experimental array compared to a control array. ESTs and genes with low reliability (detection p-value > 0.05) were discarded from the data. A > 1.5-fold increase or decrease in expression was used as criteria for a meaningful change in gene expression between the ENU-treated and control groups.

RESULTS

Cell Cycle Analysis by Laser Scanning Cytometer

An accumulation of cells in the S-phase and an increase in the number of apoptotic cells (cells with sub-G1 DNA content) were observed immediately after the administration of ENU as also observed in a previous study (Katayama et al., 2005). The number of cells in the S-phase peaked at 6 hr and that of apoptotic cells peaked at 12 hr after the treatment. Apoptosis and cell cycle alteration returned to the control lever at 48 hr after the treatment (Fig. 1). Some of the fetuses were also analyzed histopathologically using hematoxylin and eosin-stained sections and found an increase in the number of apoptotic cells in ENU-administered fetuses as also observed in a previous study (Katayama et al., 2001; data not shown).

Microarray Analysis

From the cell cycle analysis, two time points were selected for microarray analysis. It was anticipated that genes involved in apoptosis and cell cycle arrest would be identified at 6 hr after the treatment (injury phase) and genes involved in regeneration and carcinogenesis would be identified at 24 hr after the treatment (recovery phase). Up-regulated and down-regulated genes at each time point are presented in Tables 1–4.

At 6 hr after the treatment (injury phase), up-regulation of p53 target genes (p21, cyclin G1, Mdm2, and Bax) was detected as also observed in a previous study (Table 1) (Katayama et al., 2002). The tumor suppressor p53 has been implicated in the cellular responses to DNA-damaging agents. In response to DNA damage, p53 is up-regulated and transactivates a series of genes involved in the induction of apoptosis, cell cycle arrest and DNA repair (Ko and Prives, 1996). It has been shown that neuroepithelial cell apoptosis and cell cycle arrest induced by ENU are also mediated by the regulation of p53 and p53 target genes (Leonard et al., 2001; Katayama et al., 2002, 2005). The data from the present study further confirmed the involvement of p53 and its transcriptional target genes in ENU-induced neuroepithelial cell apoptosis and cell cycle arrest. These data also demonstrate the high reliability of the present microarray analysis. In addition, increased expression of other genes involved in cell cycle control (retinoblastoma protein and PCNA) and DNA repair (O^6-methylguanine-DNA methyltransferase) and decreased expression of cholesterol biosynthesis-related genes (liver stearyl-coenzyme A desaturase, cytosolic 3-hydroxy 3-methylglutaryl coenzyme A synthase, squalene synthase, growth-response protein [CL-6]) were detected (Tables 1, 2).

At 24 hr after the treatment (recovery phase), up-regulation of genes involved in cell proliferation (cyclin D1, IgE binding protein, Id1.25 and Id3a) was detected (Table 3). Cyclin D1 plays a central role in the cell cycle transition through G1 to S phase (Sherr and Roberts, 1999). IgE binding protein, also called as galectin-3, is involved in the regulation of Wnt/β-catenin signaling pathway (Shimura et al., 2004). Id proteins are

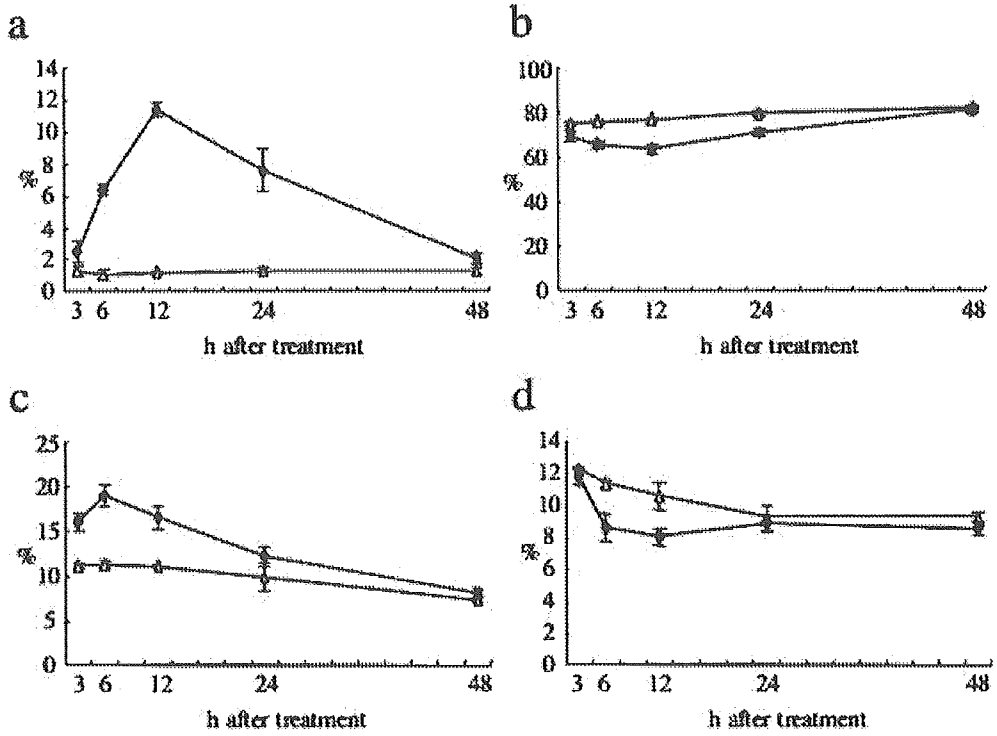

Fig. 1. Cell cycle analysis of cells isolated from fetal telencephalon after the ENU administration. Cells were isolated from fetal telencephalon and stained with propidium iodide and cell cycle phase analysis was carried out by laser scanning cytometer. Percentages for sub-G1 (a), G0/G1 (b), S (c), and G2/M (d) phases. △, control group; ◆, ENU-treated group. Percentages for each cell cycle phase are presented as the mean±SD of three dams.

Table 1
Up-Regulated Genes at 6 Hr After the ENU Treatment (Injury Phase)

	Fold Change	Accession Number
Apoptosis, cell cycle control		
p21 (cip1)	10.05±7.05	L41275
Cyclin G1	6.41±0.06	X70871
Mdm2	1.93±0.39	AA875509
Retinoblastoma protein	1.93±0.37	D25233
Bax	1.66±0.22	S76511
rBax alpha	1.65±0.23	U49729
Proliferating cell nuclear antigen (PCNA)	1.64±0.26	M24604
DNA repair, replication, transcription		
DNA primase small subunit	1.55±0.27	U67994
O^6-methylguanine-DNA methyltransferase	1.53±0.26	M76704
Metabolism		
Epoxide hydrolase	3.44±2.54	M26125
Peroxisome forming factor	2.15±0.52	E03344
UDP-glucose:ceramide glycosyltransferase	1.67±0.33	AF0477007
Pyruvate dehydrogenase phosphatase isoenzyme 1	1.59±0.16	AF062740
Phospholipase A-2-activating protein (plap)	1.59±0.01	U17901
Signal transduction		
Extracellular signal-related kinase (ERK3)	1.71±0.59	M64301
Extracellular matrix-related		
Lumican	2.01±1.02	X84039
Others		
5S rRNA	2.85±0.83	X83747
Beta-1,2-N-acetylglucosuminyltransferase II (Gnt II)	2.26±0.82	U21662
Chromogranin B (Chgb)	1.80±0.12	AF019974
Latexin	1.56±0.24	X76985
Cyclophilin	1.52±0.41	M19533

Fold changes are expressed as the mean±SD of two experiments.

Table 2
Down-Regulated Genes at 6 Hr After the ENU Treatment (Injury Phase)

	Fold Change	Accession Number
Metabolism		
Liver stearoyl-CoA desaturase	−2.02±0.29	J02585
Cytosolic 3-hydroxy 3-methylglutaryl coenzyme A synthase (EC 4.1.3.5)	−1.63±0.25	X52625
Squalene synthetase	−1.56±0.18	M95591
Others		
Growth-respons protein (CL-6)	−1.91±0.29	L13619
Pituitary tumor transforming gene (PTTG)	−1.51±0.08	U73030

Fold changes are expressed as the mean±SD of two experiments.

Table 3
Up-Regulated Genes at 24 Hr After the ENU Treatment (Recovery Phase)

	Fold Change	Accession Number
Apoptosis, cell cycle control		
Cyclin G1	4.24±0.02	X70871
Cyclin D1	1.52±0.27	D14014
DNA repair, replication, transcription		
Inhibitor of DNA-binding, splice variant Id1.25	1.59±0.24	L23148
Id3a	1.51±0.44	AF000942
Metabolism		
Epoxide hydrolase	3.83±2.81	M26125
Long chain acyl-CoA dehydrogenase (LCAD)	1.62±0.24	J05029
Signal transduction		
Type II cAMP-dependent protein kinase regulatory subunit	1.98±0.73	M12492
Serum and glucocorticoid-regulated kinase (sgk)	1.59±0.33	L01624
Cytoskeleton		
Alpha-internexin	2.08±0.51	M73049
Alpha actinin	1.54±0.33	U19893
Extracellular matrix-related		
Osteopontin	2.59±0.08	M14656
SPARC	1.60±0.62	U75929
Others		
IgE binding protein	6.83±6.01	J02962
ASM15	1.59±0.20	X59864
Stannin	1.54±0.39	M81639

Fold changes are expressed as the mean±SD of two experiments.

transcriptional factors and inhibit cell differentiation and promote proliferation (Ruzinova and Benezra, 2003). It is reasonable to consider that cell cycle progression is accelerated to compensate for the lost populations in the recovery phase. Although their precise roles have not been clarified yet, the expression of two transcriptional factors (NF1-X1 and LIM homeodomain protein [LH-2]) and a member of Rab subfamily of small GTPases (RAB 14) decreased (Table 4).

Table 4
Down-Regulated Genes at 24 Hr After the ENU Treatment (Recovery Phase)

	Fold Change	Accession Number
DNA repair, replication, transcription		
NP1-X1	−1.81±0.21	AB012234
LIM homeodomain protein (LH-2)	−1.51±0.12	L06804
Signal transduction		
RAB14	−1.63±0.29	M83680

Fold changes are expressed as the mean±SD of two experiments.

DISCUSSION

Studies have shown that from gestational Day 12 to 13, about 70% of mouse telencephalic cells are neuroepithelial cells (D'Sa-Eipper and Roth, 2000); therefore, the results from our cell cycle and microarray analyses are considered to represent mainly the changes in the cell cycle distribution and gene expression in neuroepithelial cells.

ENU alkylates mainly the O^6 position of guanine (Shibuya and Morimoto, 1993), and O^6-alkylguanine induces GC-AT transitions. O^6-methylguanine-DNA methyltransferase plays an important role in the elimination of DNA ethyl adducts (Bronstein et al., 1992), and its expression was elevated in the injury phase. However, the brain eliminates O^6-alkylguanine at a much lower

rate than other organs, and the long-term retention of O^6-alkylguanine in the brain is thought to be the cause of brain neoplasms (Koestner, 1990). It is reported that DNA excision repair and O^6-methylguanine-DNA methyltransferase are necessary for the removal of O^6-alkylguanine (Bronstein et al., 1992). Thus, it is possible that DNA excision repair does not work well in the fetal CNS and requires further evaluation.

Cholesterol metabolism plays an essential role in neural development (Farese and Herz, 1998), and squalene synthase deficient mice exhibit defective neural tube closure (Tozawa et al., 1999). In injury phase, several enzymes required for cholesterol biosynthesis (liver stearyl-coenzyme A desaturase, cytosolic 3-hydroxy 3-methylglutaryl coenzyme A synthase, squalene synthase) were down-regulated. In addition, the expression of growth-response protein (CL-6), which is also known to be involved in cholesterol homeostasis (Janowski, 2002), decreased. Decreased expression of these genes including squalene synthase may have some important roles in the abnormal development of the CNS caused by the ENU administration (Katayama et al., 2000).

In the recovery phase, the expression of two Id genes was elevated. Id proteins act as dominant negative antagonists of the basic helix-loop-helix (bHLH) family of the transcription factors, which positively regulate differentiation in many cell lineages (Ruzinova and Benezra, 2003). bHLH factors are also known to have important roles in cell fate decisions during corticogenesis (Ross et al., 2003). In the developing CNS, Id proteins are expressed in neuroepithelial cells (Jen et al., 1997), and thought to maintain neuroepithelial cells in an undifferentiated state by inhibiting bHLH factors (Ross et al., 2003; Iavarone and Lasorella, 2004). Id proteins are also expressed in astrocytic tumors, and the degree of expression of Id proteins well correlates with the grade of tumor malignancy (Vandeputte et al., 2002; Iavarone and Lasorella, 2004). The results from the present study further support the importance of bHLH factors in neurogenesis and suggest that Id proteins work to maintain neuroepithelial cells in a proliferative state to recover the lost populations.

In addition, the expression of osteopontin was prominently elevated in the recovery phase. Osteopontin is expressed in macrophages of the developing brain and contribute to their migration and phagocytic function (Choi et al., 2004). At 24 hr after the ENU administration, the number of apoptotic cells began to decrease and phagocytosis of apoptotic cells was observed frequently (Fig. 1) (Katayama et al., 2001). It is suggested that osteopontin plays an important role in the elimination of apoptotic cells by phagocytosis in the fetal CNS.

In the injury and recovery phases, the up-regulation of genes involved in the drug metabolism was detected. Among them, the expression of epoxide hydrolase prominently increased in both the phases. Epoxide hydrolase is known to play an important role in the detoxification of some DNA-damaging agents (Herrero et al., 1997). Although it is still controversial that fetal CNS really has the drug metabolizing activity, drug metabolizing enzymes are induced after the ENU administration at least in the mRNA level.

In the present study, the up-regulation of 21 genes in injury and 15 genes in recovery phases and down-regulation of 5 genes in injury and 3 genes in recovery phases were identified. Some of these genes are already known to play an important role in the injury and recovery of CNS, but others are not. Despite the precise involvement of these genes and functions need to be elucidated, the data presented here will aid in the identification of genes that play a significant role in the cell death and proliferation of neuroepithelial cells. The results from the present study will provide a better understanding of the mechanisms of development, regeneration and carcinogenesis of CNS as well as the mechanisms of ENU-induced fetal CNS injury and recovery.

ACKNOWLEDGMENTS

We thank Mr. K. Nakayama (Olympus, Tokyo, Japan) for his technical support in laser scanning cytometer. We also thank Dr. K. Imakawa, Dr. K. Baba and Dr. C. Hashizume (Graduate School of Agricultural and Life Sciences, The University of Tokyo) for their assistance in microarray analysis. This study was financially supported by the Japan Society for the Promotion of Science.

REFERENCES

Bronstein SM, Hooth MJ, Swenberg JA, Skopek TR. 1992. Modulation of ethylnitrosourea-induced toxicity and mutagenicity in human cells by O^6-benzylguanine. Cancer Res 52:3851–3856.

Choi JS, Cha JH, Park HJ, Chung JW, Chun MH, Lee MY. 2004. Transient expression of osteopontin mRNA and protein in amoeboid microglia in developing rat brain. Exp Brain Res 154:275–280.

D'Sa-Eipper C, Roth KA. 2000. Caspase regulation of neuronal progenitor cell apoptosis. Dev Neurosci 22:116–124.

Farese RV, Herz J. 1998. Cholesterol metabolism and embryogenesis. Trends Genet 14:115–120.

Herrero ME, Arand M, Hengstler JG, Oesch F. 1997. Recombinant expression of human microsomal epoxide hydrolase protects V79 Chinese hamster cells from styrene oxide- but not from ethylene oxide-induced DNA strand breaks. Environ Mol Mutagen 30: 429–439.

Iavarone A, Lasorella A. 2004. Id proteins in neural cancer. Cancer Lett 204:189–196.

Jang T, Litofsky NS, Smith TW, Ross AH, Recht LD. 2004. Aberrant nestin expression during ethylnitrosourea-(ENU)-induced neurocarcinogenesis. Neurobiol Dis 15:544–552.

Janowski BA. 2002. The hypocholesterolemic agent LY295427 up-regulates INSIG-1, identifying the INSIG-1 protein as a mediator of cholesterol homeostasis through SREBP. Proc Natl Acad Sci USA 99:12675–12680.

Jen Y, Manova K, Benezra R. 1997. Each member of the Id gene family exhibits a unique expression pattern in mouse gastrulation and neurogenesis. Dev Dyn 208:92–106.

Katayama K, Ishigami N, Suzuki M, Ohtsuka R, Kiatipattanasakul W, Nakayama H, Doi K. 2000. Teratologic studies on rat perinates and offspring from dams treated with ethylnitrosourea (ENU). Exp Anim 49:181–187.

Katayama K, Uetsuka K, Ishigami N, Nakayama H, Doi K. 2001. Apoptotic cell death and cell proliferative activity in the rat fetal central nervous system from dams administered with ethylnitrosourea (ENU). Histol Histopathol 16:79–85.

Katayama K, Ohtsuka R, Takai H, Nakayama H, Doi K. 2002. Expression of p53 and its transcriptional target genes mRNAs in the ethylnitrosourea-induced apoptosis and cell cycle arrest in the fetal central nervous system. Histol Histopathol 17:715–720.

Katayama K, Ueno M, Yamauchi H, Nagata T, Nakayama H, Doi, K. 2005. Ethylnitrosourea induces neuroepithelial cell apoptosis after S phase accumulation in a p53-dependent manner. Neurobiol Dis 18:218–225.

Ko LJ, Prives C. 1996. p53: puzzle and paradigm. Genes Dev 10: 1054–1072.

Koestner A. 1990. Characterization of N-nitrosourea-induced tumors of the nervous system; their prospective value for studies of neurocarcinogenesis and brain tumor therapy. Toxicol Pathol 18:186–192.

Leonard JR, D'Sa-Eipper C, Klocke BJ, Roth KA. 2001. Neural precursor cell apoptosis and glial tumorigenesis following transplacental ethylnitrosourea exposure. Oncogene 20:8281–8286.

Ross SE, Greenberg ME, Stiles CD. 2003. Basic helix-loop-helix factors in cortical development. Neuron 39:13–25.

Ruzinova MB, Benezra R. 2003. Id proteins in development, cell cycle and cancer. Trends Cell Biol 13:410–418.

Sherr CJ, Roberts JM. 1999. CDK inhibitors: positive and negative regulators of G1-phase progression. Genes Dev 13:1501–1512.

Shibuya T, Morimoto K. 1993. A review of genotoxicity of 1-ethyl-1-nitrosourea. Mutat Res 297:3–38.

Shimura T, Takenaka Y, Tsutsumi S, Hogan V, Kikuchi A, Raz A. 2004. Galectin-3, a novel binding partner of β-catenin. Cancer Res 64: 6363–6367.

Tozawa R, Ishibashi S, Osuga J, Yagyu H, Oka T, Cheng Z, Ohashi K, Perrey S, Shionoiri F, Yahagi N, Harada K, Gotoda T, Yazaki Y, Yamada N. 1999. Embryonic lethality and defective neural tube closure in mice lacking squalene synthase. J Biol Chem 274: 30843–30848.

Vandeputte DA, Troost D, Leenstra S, Ijlst-Keizers H, Ramkema M, Bosch DA, Baas F, Das NK, Aronica E. 2002. Expression and distribution of id helix-loop-helix proteins in human astrocytic tumors. Glia 38: 329–338.

Yoshikawa K. 2000. Cell cycle regulators in neural stem cells and postmitotic neurons. Neurosci Res 37:1–14.

Available online at www.sciencedirect.com

SCIENCE DIRECT

ELSEVIER

Experimental and Molecular Pathology 79 (2005) 59 – 67

Experimental and Molecular Pathology

www.elsevier.com/locate/yexmp

Hydroxyurea (HU)-induced apoptosis in the mouse fetal lung

Gye-Hyeong Woo[a], Eun-Jung Bak[b], Hiroyuki Nakayama[a], Kunio Doi[a,*]

[a]*Department of Veterinary Pathology, Graduate School of Agricultural and Life Sciences, The University of Tokyo, 1-1-1 Yayoi, Bunkyo-ku, Tokyo 113-8657, Japan*

[b]*Department of Biomedical Science, Graduate School of Agricultural and Life Sciences, The University of Tokyo, Japan*

Received 10 February 2005
Available online 22 April 2005

Abstract

In this study, the cytotoxicologic effects of HU on the fetal lung were assessed by exposing pregnant mice to HU on day 13 of gestation. The number of TUNEL-positive cells, i.e., apoptotic cells, in the fetal lung began to increase at 3 h after treatment (h), peaked at 6 h, and decreased thereafter, and the sequence of the number of cleaved caspase 3-positive cells corresponded to that of TUNEL-positive cells. Such positive reactivity for TUNEL and cleaved caspase 3 was mainly seen in pulmonary mesenchymal cells. Prior to the induction of apoptosis, the number of p53-positive cells in the fetal lung prominently increased at 1 and 3 h, and decreased thereafter. Among p53 transcriptional target genes (*p21*, *fas*, *bax*, *apaf1*, *cyclin G*, *mdm2*, and *gad 45*) examined, the expression levels of *p21*, *bax*, and *cyclin G* mRNAs were significantly elevated. In addition, the expression of *fas* mRNA tended to show higher levels compared with controls until 24 h. In addition, the results of flow cytometric analysis suggested that cell cycle arrest might be induced in S phase at 3 h. The present results suggest that HU-induced apoptosis in the mouse fetal lung may be closely related with the induction of p53.

Keywords: Apoptosis; p53; Cell cycle arrest; Hydroxyurea; Mouse metus; Lung

Introduction

Hydroxyurea (HU), a potent mammalian teratogen, rapidly kills proliferating embryonic cells and also inhibits DNA synthesis. In experimental animals, there are many reports of HU-related teratogenic effects. For example, HU induces anomalies in the central nervous system, craniofacial tissues, skull, and limbs (Barr and Beaudoin, 1981; Butcher et al., 1973). In human beings, monitoring of adverse effects of HU has shown fever, pulmonary toxicity including neonatal respiratory distress, and dermatotoxicity (Hennemann et al., 1993; Hirri and Green, 2001; Jackson et al., 1990; Thauvin-Robinet et al., 2001). We previously reported that HU administration to pregnant mice on day 13 of gestation induced a marked apoptosis in neuroepithelial cells in the CNS, and mesenchymal cells in the lung, craniofacial tissues, and limb buds. Therefore, we suggested that such excess cell death in the fetal tissues may have a certain relation to the later occurrence of morphological or functional abnormalities reported in these tissues following HU administration (Woo et al., 2003).

Apoptosis is a particular form of cell death characterized by chromatin condensation, cell membrane blebbing, and fragmentation of nuclei. It is involved in pathological situations by diseases and toxic insults (Bursch et al., 1992; Vaux et al., 1994), as well as embryogenesis and maintenance of many adult tissues (Duvall and Wyllie, 1986; Saunders, 1966). It has been reported that apoptosis is intimately related with the p53 tumor suppressor gene. p53 plays a crucial role in cell cycle arrest, apoptosis, or senescence in response to DNA damage and other cellular stresses (Ko and Prives, 1996; Levine, 1997; Vogelstein et al., 2000; Vousden, 2000). It has been shown that cell response by p53 is largely due to its ability to transcriptionally activate genes that directly control cell fate (Ko and Prives, 1996; Levine, 1997; Vogelstein et al., 2000).

After it was shown that HU inhibited DNA synthesis without immediate effect on RNA or protein synthesis

* Corresponding author. Fax: +81 3 5841 8185.
E-mail address: akunio@mail.ecc.u-tokyo.ac.jp (K. Doi).

0014-4800/$ - see front matter © 2005 Elsevier Inc. All rights reserved.
doi:10.1016/j.yexmp.2005.02.007

(Yarbro et al., 1965), ribonucleotide reductase was identified as the target enzyme of HU in a cell-free bacterial system (Krakoff et al., 1968). This enzyme was inactivated and DNA synthesis was selectively inhibited, resulting in cell death in S phase (Yarbro, 1992). However, the mechanisms of cell death after HU-induced DNA damage have not been elucidated in vivo.

In this study, we investigated the sequential changes in the development of apoptosis and in the expression of apoptosis-related genes and proteins in the fetal lung in order to elucidate molecular genetic regulatory mechanisms of HU-induced apoptosis in the fetal lung. The protocol of the present study was approved by the Animal Use and Care Committee of the Graduate School of Agricultural and Life Sciences, the University of Tokyo.

Materials and methods

Animals

Eighty-four 8-week-old pregnant mice of the Crj:CD-1 (ICR) strain were obtained from Charles River Japan Co., Yokohama, Japan. They were kept in an animal room under controlled conditions (temperature, 23 ± 2°C; relative humidity, 55 ± 5%) using an isolator caging system (Niki Shoji, Co., Tokyo) and were fed commercial pellets (MF, Oriental Yeast Co., Tokyo) and water ad libitum.

Chemicals

Hydroxyurea (HU) (Sigma, St. Louis, MO) was dissolved in distilled water immediately before the treatment, and the concentration was adjusted to 60 mg/ml. 5-Bromo-2′-deoxyuridine (BrdU; Sigma, St. Louis, MO) was also dissolved in physiologic saline immediately before the treatment, and the concentration was adjusted to 4 mg/ml.

Treatments

Forty-eight pregnant mice were injected with 400 mg/kg b.w. of HU intraperitoneally (i.p.) on day 13 of gestation, and 8 dams each were sacrificed by heart puncture under ether anesthesia at 1, 3, 6, 12, 24, and 48 h after the treatment (h). Another thirty-six pregnant mice were injected i.p. with distilled water, and six dams each were sacrificed in the same way. Twenty mg/kg b.w. of BrdU was injected i.p. to 5 dams of the HU-treated group killed at each time point and to 3 dams of the control group for histopathology, immunohistochemistry, and reverse transcriptase-polymerase chain reaction (RT-PCR) at 1 h before necropsy, and together with HU to 3 dams of the HU-treated group killed at each time point and to 3 dams of the control group for flow cytometry, respectively.

Histopathology

Fetuses were collected by caesarian section and fixed in 10% neutral-buffered formalin. Paraffin sections (4 μm) were stained with hematoxylin and eosin (HE). Some of the paraffin sections were subjected to in situ detection of fragmented DNA and to immunohistochemical staining for TUNEL, BrdU, p53, and cleaved caspase 3 as mentioned below.

In situ detection of fragmented DNA

DNA fragmentation was examined on paraffin sections using the modified terminal deoxynucleotidyltransferase-mediated dUTP end labeling (TUNEL) method first proposed by Gravieli et al. (1992), with a commercial apoptosis detection kit (ApopTag In situ Apoptosis Detection Kit; Oncor, Gaithersburg, MD). In brief, the procedure was as follows: multiple fragmented 3′-OH ends were labeled with digoxigenin-dUTP in the presence of terminal deoxynucleotidyl transferase (TdT). Peroxidase-conjugated anti-digoxigenin antibody was then reacted with the sections. Apoptotic nuclei were visualized using the peroxidase-diaminobenzidine (DAB) reaction. The sections were then counterstained with methyl green. TUNEL-positive cells in the lung were counted under a light microscope (×400). The number of TUNEL-positive cells/mm^2 was expressed as the mean ± standard deviation (SD) for 5 dams (5 fetuses/dam) at each time point of examination.

Immunohistochemistry

For the detection of BrdU, paraffin sections were treated with 0.1% trypsin and 0.1% calcium chloride in Tris buffer at 37°C and 1 N HCl at room temperature (RT) for 30 min each. After washing in tris-buffered saline (TBS), endogenous peroxidase activity was quenched for 30 min in 0.3% H_2O_2 in methanol, followed by 3 washes with TBS. The sections were incubated in 8% skim milk for 40 min at 37°C to reduce non-specific reaction, and immediately replaced with mouse antibody against BrdU (1:100; Dako) in TBS at 4°C and then incubated overnight at 4°C. After washing in TBS, the sections were incubated with biotinylated antibody against mouse IgG (1:400; Kirkegaard and Perry, Gaitherburg, MD) according to the manufacturer's instructions, washed in TBS, and then incubated with streptavidin (1:300; Dako).

For the detection of p53, sections were immersed in 10 mM citrate buffer, pH 6.0, and autoclaved for 10 min at 120°C. After washing in TBS, endogenous peroxidase activity was quenched in 0.3% H_2O_2 in methanol for 30 min, followed by 3 washes with TBS. The sections were incubated in 8% skim milk for 40 min at 37°C to reduce non-specific reaction, and immediately replaced with rabbit antibody against p53 (1:300; Santa Cruz) in TBS at 4°C and

then incubated overnight at 4°C. After washing in TBS, the sections were incubated with Envision+ kit (Dako, Carpinteria, CA) for 30 min at room temperature, and then washed in TBS.

For the detection of cleaved caspase 3, sections were immersed in 10 mM citrate buffer, pH 6.0, and autoclaved for 10 min at 120°C. After washing in TBS, endogenous peroxidase activity was quenched for 30 min in 0.3% H_2O_2 in methanol followed by 3 washes of TBS. The sections were incubated in 8% skim milk for 40 min at 37°C to reduce nonspecific reaction, and immediately replaced with rabbit antibody against cleaved caspase 3 (1:200; Cell signaling) in TBS at 4°C and then incubated overnight at 4°C. After washing in TBS, sections were incubated with biotinylated antibody against rabbit IgG (1:400; Kirkegaard and Perry, Gaitherburg, MD) according to the manufacturer's instructions, then washed in TBS and incubated with streptavidin (1:300; Dako).

The sections were visualized using the peroxidase-DAB reaction and then counterstained with methyl green. Positive cells in the lung were counted under a light microscope (×400). The number of positive cells/mm^2 was expressed as the mean ± SD for 5 dams (5 fetuses/dam) at each point of examination, and a statistical analysis was done with Student's *t* test comparing the control and HU-treated groups.

RNA extraction and RT-PCR analysis

The lungs of seven fetuses from each dam were pooled and the total cellular RNA was extracted from each homogenized sample using the Isogen kit (Nippon Gene, Toyama, Japan). The RT reaction for synthesizing the first-strand cDNA was carried out using an oligo $(dT)_{12-18}$ primer and SUPERSCRIPT™ II Rnase H$^-$ Reverse Transcriptase (Gibco, Gaithersburg, MD). PCR was performed using oligonucleotide primers sets corresponding to the cDNA sequences of *p53*'s transcriptional target genes (*p21*, *apaf-1*, *bax*, *cyclin G*, *gadd 45*, *mdm2*, and *fas*), and glyceraldehyde-3-phosphate dehydrogenase (GAPDH) (Table 1). PCR amplifications were performed in 50 μl of reaction mixture containing 5 μl 10× PCR buffer (100 mM Tris–HCl buffer, 500 mM KCl, and 15 mM $MgCl_2$; Takara, Shiga, Japan), 5 μl dNTP (Takara), 1.25 U of Taq™, 50 pM each of sense and antisense primer, and 1 μl of cDNA. After an initial denaturation at 94°C for 7 min, amplification was performed in a Takara PCR Thermal cycler SP (Takara) (Table 1) under the following conditions: 1 min of denaturation at 94°C, 2 min (*fas*) or 1 min (the others) of annealing at 64°C (*fas*) or 58.5°C (the others), and 3 min (*fas*) or 1 min (the others) of extension at 72°C. Amplification of *GAPDH* mRNA was used as the control for template concentration loading. The PCR products were electrophoretically separated in 2% agarose S (Nippon Gene) in TBE buffer (89 mM Tris-aminomethane, 89 mM Boric acid, 10 mM EDTA). The gels were stained with ethidium bromide (Gibco). Fluorescent bands were visualized using a UV-CCD video system (EpiLight$_{UVFA1100}$; AISIN COSMOS, Tokyo, Japan) and were analyzed using an image-analysis software, Quantity One (pdi, NY). The intensity of the band relative to the GAPDH band was represented as the mean ± standard error (SE). The significance of differences between the control group and HU-treated group was evaluated with Student's *t* test or Welch's *t* test.

Flow cytometry

For measuring sub-G1 DNA content, the cells were prepared in five fetal lungs of each group, washed in PBS, and resuspended in 1 ml of PBS at a density of 1×10^6 cells/ml. An amount of 2.7 ml of ice-cold ethanol was added to a final ethanol concentration of 70%. After centrifugation, the cells were resuspended in 1 ml of PBS and incubated with 10 μl of RNAse for 40 min at 37°C. An amount of 10 μl of propidium-iodide (5 mg/ml) was added. FSC and SSC analysis was performed to assess changes in cell morphology, and FL-2H analysis to detect changes in DNA content and DNA fragmentation using FACScalibur machine (Becton-Dickinson, Franklin Lakes, NJ).

Results

Histological and immunohistochemical findings

Pyknosis was observed mainly in mesenchymal cells of the lung, and it was also found in a small number of

Table 1
Oligonucleotide primers for each molecule and cycle numbers

Gene	Sense (5′–3′)	Antisense (5′–3′)	Cycle numbers
p53	GCCAGGAGACATTTTCAGGC	AACTGCACAGGGCACGTCTT	26
p21	AATCCTGGTGATGTCCGACC	GACCAATCTGCGCTTGGAGT	30
fas	GCTCAGAAGGGAAGGAGTAC	ACTGGAGGTTCTAGATTCAGG	35
bax	TTCATCCAGGATCGAGCAGG	TGAGGACTCCAGCCACAAAGAT	32
Apaf-1	GACTGTTGGACCGTGGCATT	CCAAGCCCTCGGAATCTTTC	35
mdm2	CATCAGGATCTTGACGATGGC	GGAGAAGCTAGATTCCACACTCT	30
Gadd45	AGACCGAAAGGATGGACACG	CCCACTGATCCATGTAGCGA	32
Cyclin G	CTTTGGCTTTGACACGGAGAC	GGAATCGTTGGGAGGTGAGTT	28
GAPDH	TGATGGGTGTGAACCACGAG	TTGAAGTCGCAGGAGACAACC	21

bronchial and bronchiolar epithelial cells. The number of pyknotic cells began to increase at 3 h, peaked at 6 h, and decreased at 24 h. Such pyknotic nuclei were strongly positive for TUNEL stain and cleaved caspase-3. The number of TUNEL-positive cells began to increase at 3 h, peaked at 6 h, and rapidly decreased at 24 h (Fig. 1B). The sequence of the number of cleaved caspase 3-positive cells corresponded well to that of TUNEL-positive cells (Fig. 2).

A lot of p53-positive cells were detected from 1 to 3 h (Fig. 3B). After that, p53-positive cells rapidly decreased toward 12 h and returned to the control level at 24 h (Fig. 3B).

The results of BrdU labeling of the fetal lung are shown in Figs. 4A and B. Except for at 6 h, the number of BrdU-positive cells was significantly smaller in the HU-treated group than in the control group until 24 h.

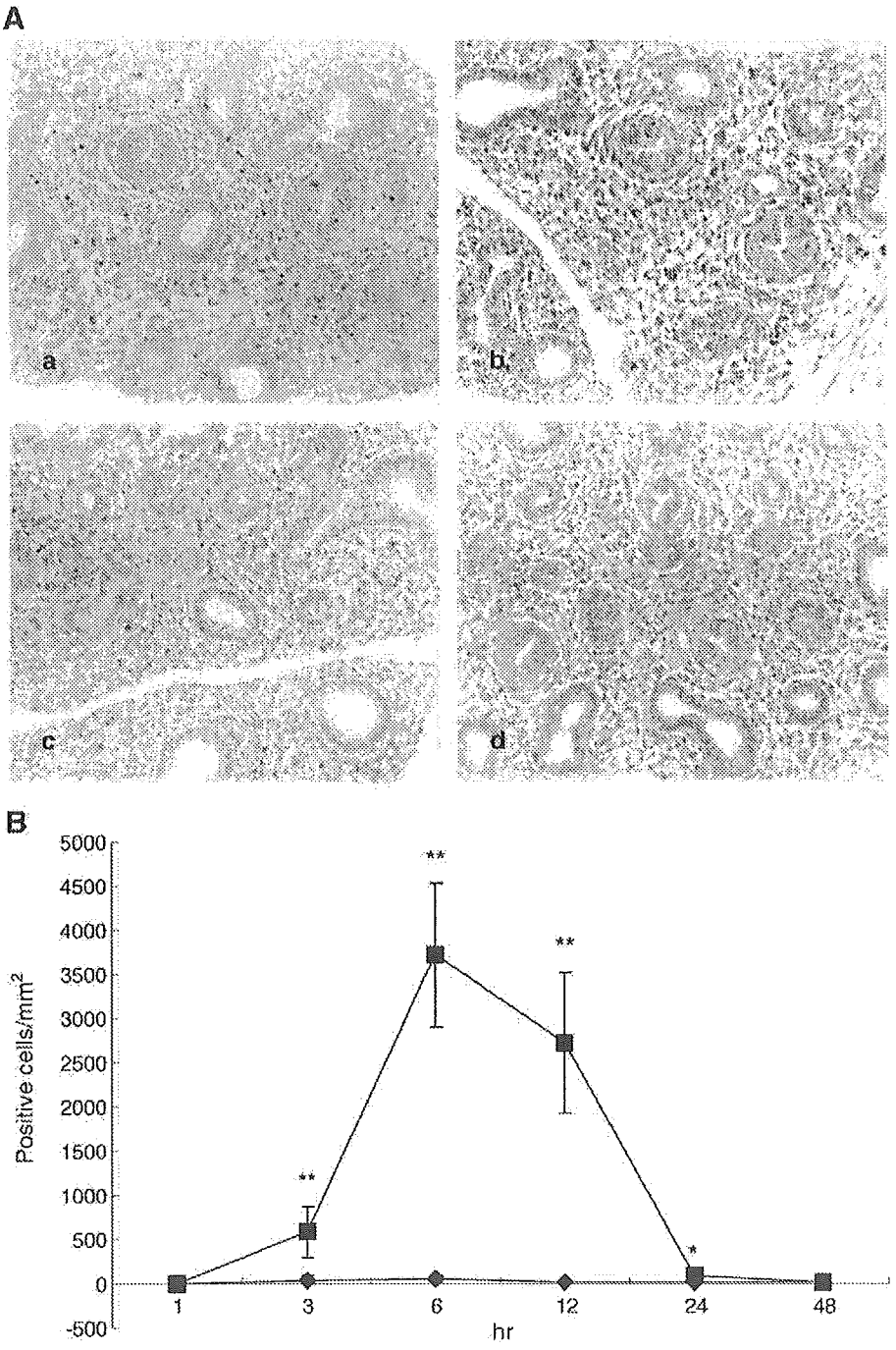

Fig. 1. Immunohistochemistry for TUNEL. (A) TUNEL-positive cells in the fetal lung of the HU-treated group at 3 (a), 6 (b), and 24 h (c), and of a fetus of the control group at 6 h (d). Immunostaining, ×300. (B) Changes in the number of TUNEL-positive cells in the fetal lung of the HU-treated group (■) and of the control group (◆). Each value represents the mean ± SD of 5 dams. *$P < 0.05$, **$P < 0.01$: significantly different from the control by Student's t test.

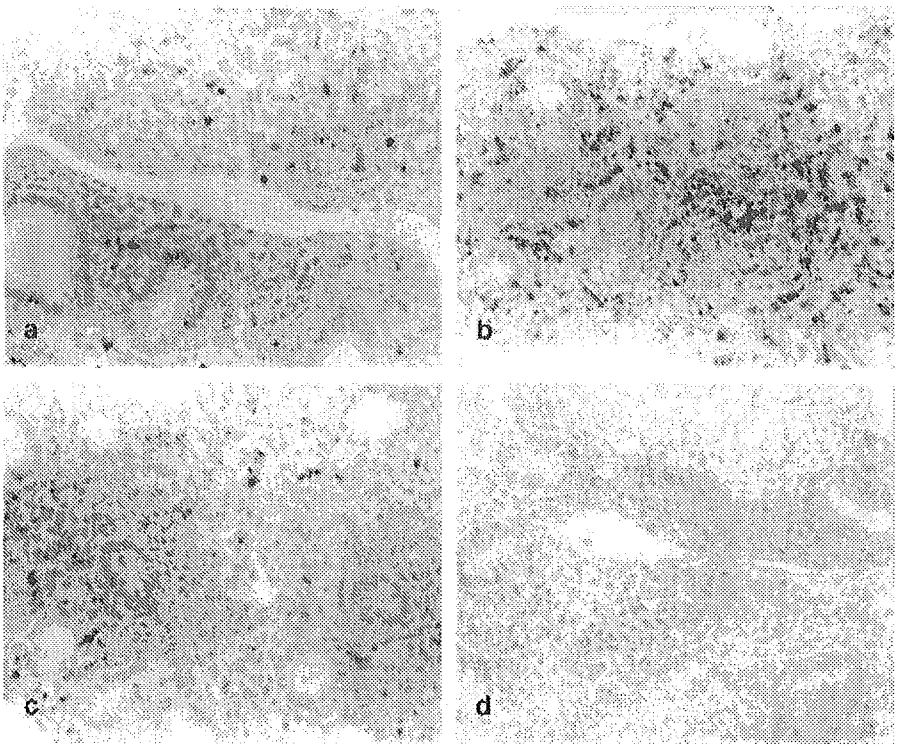

Fig. 2. Immunohistochemistry for cleaved caspase-3 in the fetal lung of the HU-treated group at 3 h (a), 6 h (b) and 12 h (c), and of the control group at 6 h (d). Immunostaining, ×300.

Changes in the expression levels of apoptosis-related genes mRNAs

The results of RT-PCR analysis for the expression levels of apoptosis- and cell cycle arrest-related gene (*p53*, *p21*, *bax*, *apaf1*, *cyclin G*, *mdm2*, *gadd 45*, and *fas*) mRNAs in the fetal lung are shown in Fig. 6. The expression level of *p21* mRNA was significantly elevated at 1 and 3 h (Fig. 5). In addition, the expression levels of *fas*, *bax*, and *cyclin G* mRNAs showed higher levels compared with those in controls (Fig. 5).

Findings of flow cytometric analysis

Flow cytometry after exposure to HU demonstrated a time-dependent appearance of DNA debris in the sub-G0/G1 region. The sub-G0/G1 fraction rapidly increased at 3 h, peaked at 6 h, and decreased thereafter (Fig. 6). The S-phase fraction also slightly increased at 3 h and decreased at 6 h, although the G2/M fraction drastically decreased at 3 h (Fig. 6).

Discussion

In our previous studies, an increased apoptosis was detected in the lung of fetuses from pregnant mice administrated with HU on day 13 of gestation, suggesting that such excess cell death in the fetal lung might have a certain relation to a significant decrease in the lung weight of neonates (Woo et al., 2003, 2004). In human beings, as mentioned before, side effects of HU on the lung such as acute alveolitis (Hennemann et al., 1993) and neonatal respiratory distress (Thauvin-Robinet et al., 2001) have been reported.

In the present study, the sequential changes in the expression of p53 and its transcriptional target genes (*p21*, *apaf-1*, *bax*, *cyclin G*, *gadd 45*, *mdm2*, and *fas*) were examined in the fetal mouse lung from dams treated with HU, because p53 has been known to play an important role in the induction of apoptosis (Lakin and Jackson, 1999). It has been reported that p53 binds to DNA in a sequence-specific manner (Kern et al., 1991) and regulates the transcription of gene products involved in growth arrest, DNA repair, apoptosis, and inhibition of angiogenesis (Farmer et al., 1992; Pietenpol et al., 1994; Zambetti et al., 1992). In the present study, p53-positive cells were observed in many mesenchymal cells and a small number of epithelial cells prior to the induction of apoptosis. This indicates that HU-induced apoptosis in the fetal lung is dependent on p53.

p53-induced apoptosis is proposed to be mediated by transactivation of *bax* (Miyashita and Reed, 1995), *fas/APO1* (Owen-Scaub et al., 1995), and p53-inducible genes (Polyak et al., 1997). Significant elevation of *bax* mRNA expression was seen at 6 h and 12 h. The *bax* mRNA expression is upregulated during p53-dependent apoptosis (Miyashita and Reed, 1995), and bax accelerates release of

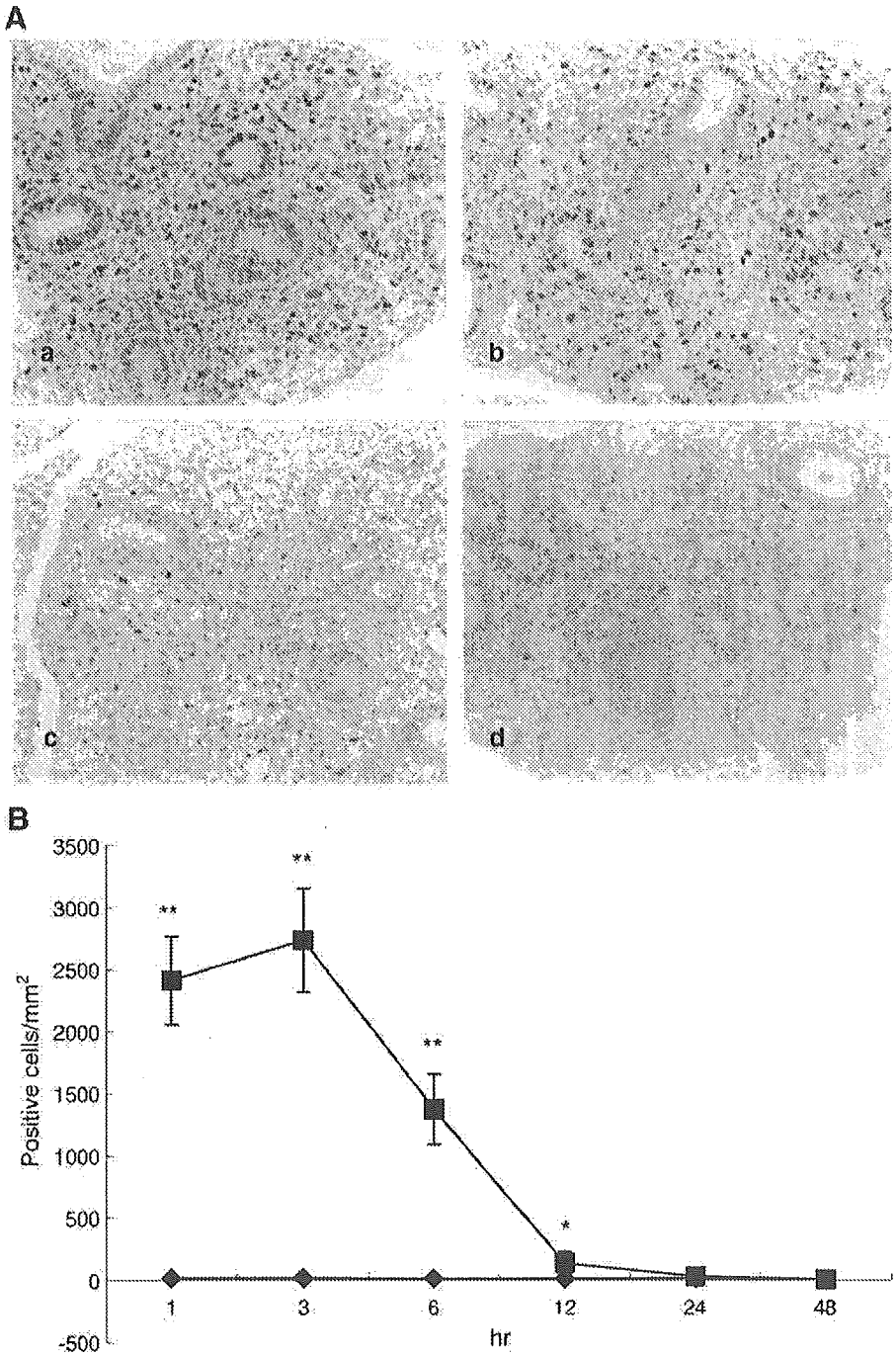

Fig. 3. Immunohistochemistry for p53. (A) p53-positive cells in the fetal lung of the HU-treated group at 1 (a), 3 (b), and 12 h (c), and of the control group at 3 h (d). Immunostaining, ×300. (B) Changes in the number of p53-positive cells in the fetal lung of the HU-treated group (■) and of the control group (◆). Each value represents the mean ± SD of 5 dams. $*P < 0.05$, $**P < 0.01$: significantly different from the control by Student's t test.

the apoptosis-inducing factors and cytochrome *c* from mitochondria, thus activating the caspase cascade (Sionov and Haupt, 1999). In addition, caspase activation was identified by immunohistochemistry on cleaved caspase 3. The apoptotic activity of bax is directly implicated in tumor suppression, as *bax* mutations have been observed in human colon tumors (Rampino et al., 1997; Yin et al., 1997). Further, *bax* expression in breast cancer cell lines expressing wild-type p53 increased apoptotic cells after exposure to genotoxic agents, demonstrating an importance of bax activation in p53-dependent apoptosis (Wagener et al., 1996).

Although not significant, an increase in the *fas* mRNA expression was observed throughout the experimental period compared with the control group. This suggests an important participation of the fas/CD95-fasL receptor–

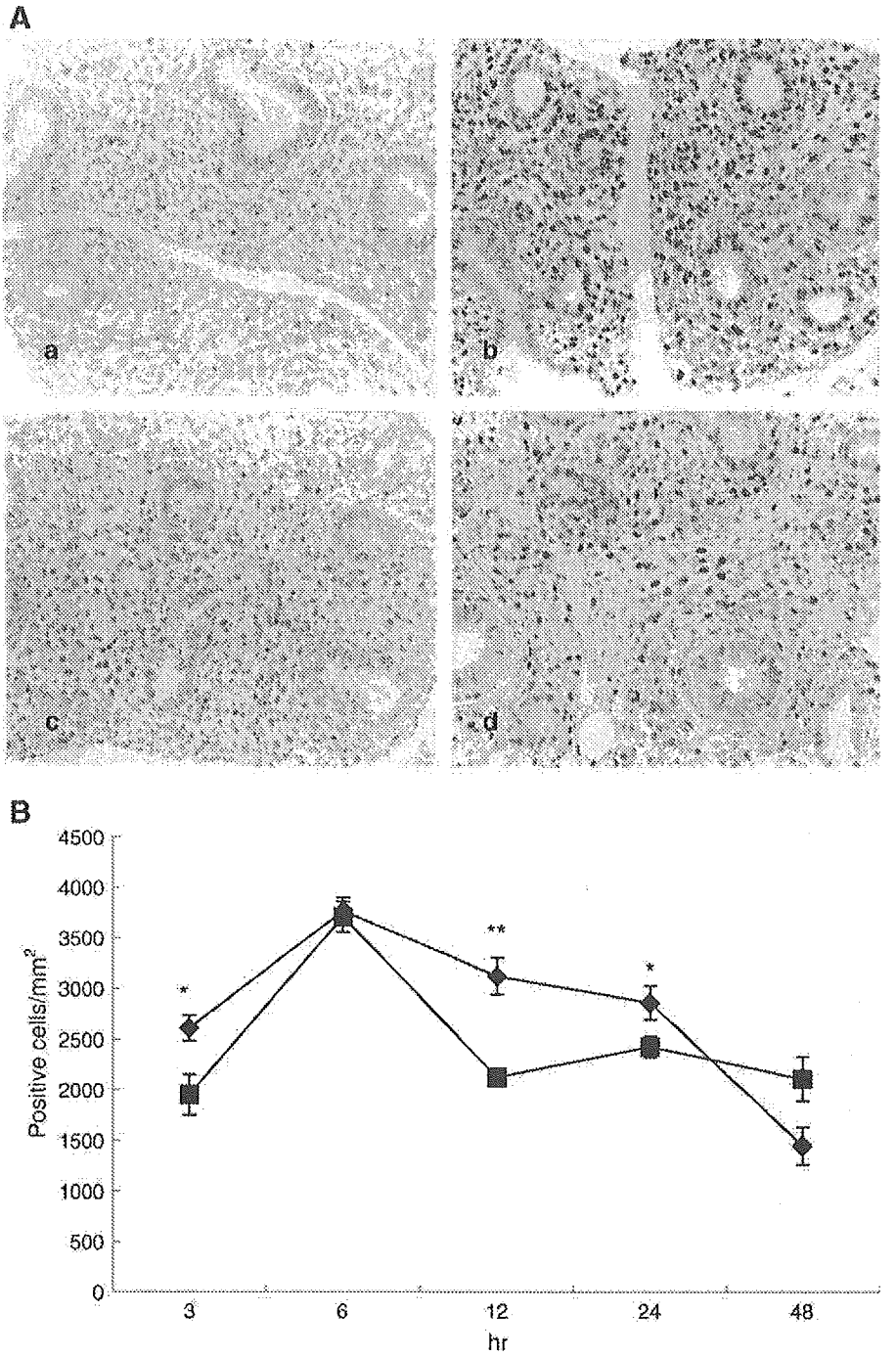

Fig. 4. Immunohistochemistry for BrdU. (A) BrdU-positive cells in the fetal lung of the HU-treated group at 3 (a), 6 (b), and 12 h (c), and of the control group at 6 h (d). Immunostaining, ×300. (B) Changes in the number of BrdU-positive cells in the fetal lung of the HU-treated group (■) and of the control group (◆). Each value represents the mean ± SD of 5 dams. *$P < 0.05$, **$P < 0.01$: significantly different from the control by Student's t test.

ligand system in HU-induced apoptosis. The fas/CD95 death receptor loci as well as the gene encoding for fas ligand are direct targets of p53 (Maecker et al., 2000; Muller et al., 1998; Owen-Scaub et al., 1995).

The expression of *cyclin G* mRNA was significantly elevated from 3 to 6 h compared with the control group. In this connection, it was reported that cyclin G has growth-promoting functions (Reimer et al., 1999; Smith et al., 1997). *Gadd 45* is one of the target genes of the transcription factor p53, and gadd 45 is involved in DNA repair (Smith et al., 1994). However, there were no changes in gadd 45 mRNA expression in the present study.

In our study, the elevation of *p21* mRNA expression occurred following the prominent increase in the number of immunohistochemically p53-positive cells. p21 is largely responsible for p53-dependent G1 arrest in

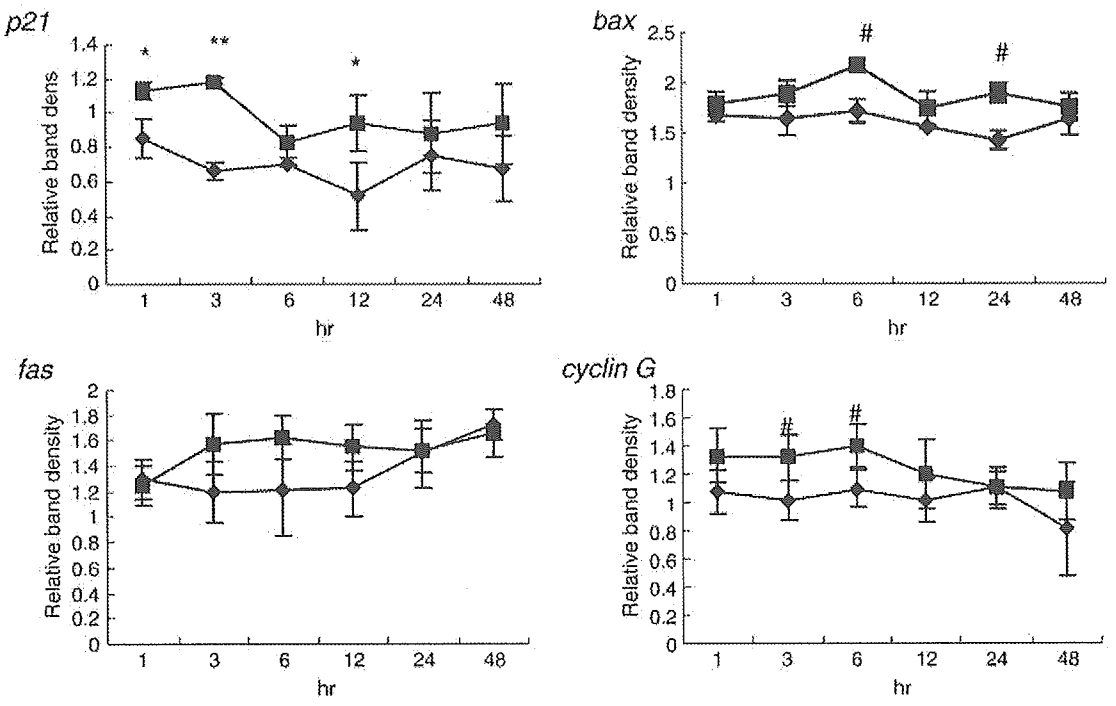

Fig. 5. Sequential changes in the expression of *p53*'s transcriptional target gene mRNAs. Each value represents the mean ± SE of 5 dams (HU-treated group) (■) and of 3 dams (control group) (◆). Glyceraldehyde-3-phosphate dehydrogenase (GAPDH) was used as an internal control. $^{*}P < 0.05$, $^{**}P < 0.01$ (Student's t test), $^{\#}P < 0.05$ (Welch's t test): significantly different from the control.

response to radiation (Dulic et al., 1994). Induction and activation of p53 lead to transcriptional induction of p21 owing to strong p53 response elements in the p21 gene promoter. The subsequent accumulation of p21 then leads to binding to and inactivation of G1 Cdks. According to the results of flow cytometric analysis, the S-phase fraction increased at 3 h and decreased thereafter, although the G2/M fraction drastically decreased at 3 h, suggesting that HU resulted in a specific accumulation of cells in the S compartment at 3 h.

In conclusion, p53 protein was expressed prior to the induction of apoptosis, and its target genes were transactivated following HU treatment. The present results totally suggest that HU-induced apoptosis in the mouse fetal lung may be closely related with the induction of p53.

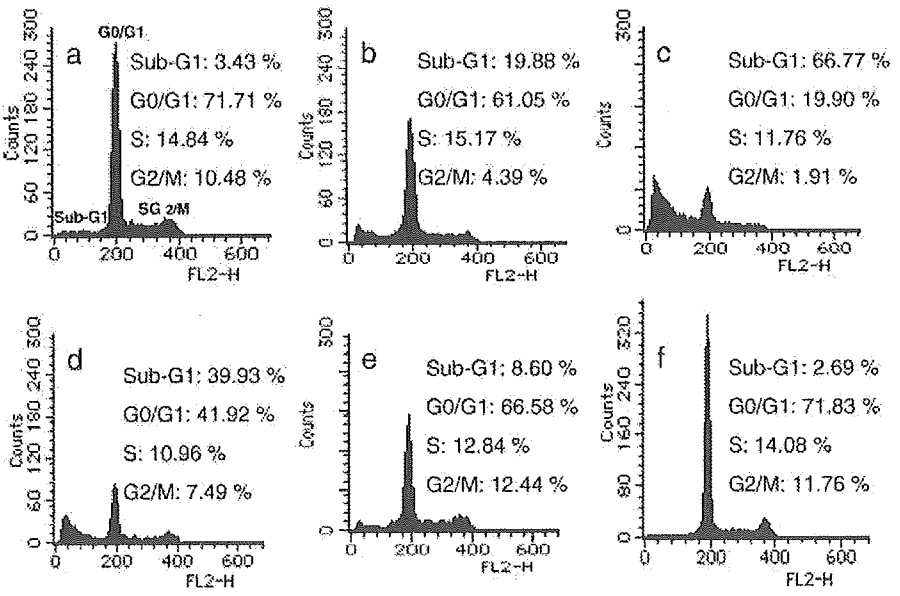

Fig. 6. Cell cycle profile in the fetal lung cells at 1 (a), 3 (b), 6 (c), 12 (d), and 24 h (e) after treatment with HU and of the control group (f). The gates for the sub-G0/G1, G0/G1, S, and G2/M phases are shown in 1 h.

References

Barr Jr., M., Beaudoin, A.R., 1981. An exploration of the role of hydroxyurea injection time in fetal growth and teratogenesis in rats. Teratology 24, 163–167.

Bursch, W., Oberhammer, F., Schulte-Hermann, R., 1992. Cell death by apoptosis and its protective role against disease. Trends Pharmacol. Sci. 13, 245–251.

Butcher, R.E., Scott, W.J., Kazhaier, K.E.J., 1973. Postnatal effects in rats of prenatal treatment with hydroxyurea. Teratology 7, 161–165.

Dulic, V., Kaufmann, W.K., Wilson, S.J., Tlsty, T.D., Lees, E., Harper, J.W., Elledge, S.J., Reed, S.I., 1994. p53-dependent inhibition of cyclin-dependent kinase activities in human fibroblasts during radiation-induced G1 arrest. Cell 76, 1013–1023.

Duvall, E., Wyllie, A.H., 1986. Death and the cell. Immunol. Today 7, 115–119.

Farmer, G., Bargonetti, J., Zhu, H., Freidman, P., Prywes, R., Prives, C., 1992. Wild-type p53 activates transcription in vivo. Nature 358, 83–85.

Gravieli, Y., Sherman, Y., Ben, S., 1992. Identification programmed cell death in situ via specific labeling of nuclear DNA fragmentation. J. Cell Biol. 119, 493–501.

Hennemann, B., Bross, K.J., Reichle, A., Andreensen, R., 1993. Acute alveolitis induced by hydroxyurea in a patient with myeloproliferative syndrome. Ann. Hematol. 67, 133–134.

Hirri, H.M., Green, P.J., 2001. Skin lesion caused by hydroxyurea. Eur. J. Haematol. 67, 328–329.

Jackson, G.H., Wallis, J., Ledingham, J., Lennard, A., Proctor, S.J., 1990. Hydroxyurea-induced acute alveolitis in a patient with chronic myeloid leukaemia. Cancer Chemother. Pharmacol. 27, 168–169.

Krakoff, I.H., Brown, N.C., Reichard, P., 1968. Inhibition of ribonucleoside diphosphate reductase by hydroxyurea. Cancer Res. 28, 1559–1565.

Kern, S.E., Kinzler, K.W., Bruskin, A., Jarosz, D., Friedman, P., Prives, C., Vogelstein, B., 1991. Identification of p53 as a sequence-specific DNA-binding protein. Science 252, 1708–1710.

Ko, L.J., Prives, C., 1996. p53: puzzle and paradigm. Genes Dev. 10, 1054–1072.

Lakin, N.D., Jackson, S.P., 1999. Regulation of p53 in response to DNA damage. Oncogene 18, 7644–7655.

Levine, A.J., 1997. p53, the cellular gatekeeper for growth and division. Cell 88, 323–331.

Maecker, H.L., Koumenis, C., Giaccia, A.J., 2000. p53 promotes selection for Fas-mediated apoptotic resistance. Cancer Res. 60, 4638–4644.

Miyashita, T., Reed, J.C., 1995. Tumor suppressor p53 is a direct transcriptional activator of the human bax gene. Cell 80, 293–299.

Muller, M., Wilder, S., Bannasch, D., Israeli, D., Lehlbach, K., Li-Weber, M., Friedman, S.L., Galle, P.R., Stremmel, W., Oren, M., Krammer, P.H., 1998. p53 activates the CD95 (APO-1/Fas) gene in response to DNA damage by anticancer drugs. J. Exp. Med. 188, 2033–2045.

Owen-Scaub, L.B., Zhang, W., Cusack, J.C., Angelo, L.S., Santee, S.M., Fujiwara, T., Roth, J.A., Deisseroth, A.B., Zhang, W.W., Kruzel, E., Radinsky, R., 1995. Wild-type human p53 and a temperature-sensitive mutant induce Fas/APO-1 expression. Mol. Cell. Biol. 15, 3032–3040.

Pietenpol, J.A., Tokino, T., El-Deiry, W.S., Kinzler, K.W., Vogelstein, B., 1994. Sequence-specific transcriptional activation is essential for growth suppression by p53. Proc. Natl. Acad. Sci. U. S. A. 91, 1998–2002.

Polyak, K., Xia, Y., Zweier, J.L., Kinzler, K.W., Vogelstein, B., 1997. A model for p53-induced apoptosis. Nature 389, 300–305.

Rampino, N., Yamamoto, H., Ionov, Y., Li, Y., Sawai, H., Reed, J.C., Perucho, M., 1997. Somatic frameshift mutations in the Bax gene in colon cancers of the microsatellite mutator phenotype. Science 275, 967–969.

Reimer, C.L., Boras, A.M., Kurdistanni, S.K., Garreau, J.R., Chung, M., Aaronson, S.A., Lee, S.W., 1999. Altered regulation of cyclin G in human breast cancer and its specific localization at replication foci in response to DNA damage in p53+/+ cells. J. Biol. Chem. 274, 11022–11029.

Saunders, J.V., 1966. Death in embryonic systems. Science 154, 604–612.

Sionov, R.V., Haupt, Y., 1999. The cellular response to p53: the decision between life and death. Oncogene 18, 6145–6157.

Smith, M.L., Chen, I.-T., Zhan, Q., Bae, I., Chen, C.-Y., Gilmer, T.M., Kastan, M.B., O'Connor, P.M., Fornace, A.J., 1994. Interaction of the p53-regulated protein Gadd45 with proliferating cell nuclear antigen. Science 266, 1376–1380.

Smith, M.L., Kontny, H.U., Bortnick, R., Fornace, A.J. Jr., 1997. The p53-regulated cyclin G gene promotes cell growth: p53 downstream effectors cyclin G and Gadd45 exert different effects on cisplatin chemosensitivity. Exp. Cell Res. 230, 61–68.

Thauvin-Robinet, C., Maingueneau, C., Robert, E., Elefant, E., Guy, H., Caillot, D., Casasnovas, R.O., Douvier, S., Nivelon-Chevallier, A., 2001. Exposure to hydroxyurea during pregnancy: a case series. Leukemia 15, 1309–1311.

Vaux, D.L., Haecker, G., Strasser, A., 1994. An evolutionary perspective on apoptosis. Cell 76, 777–779.

Vogelstein, B., Lane, D., Levine, A.J., 2000. Surfing the p53 network. Nature 408, 307–310.

Vousden, K.H., 2000. p53: death star. Cell 103, 691–694.

Wagener, C., Bargou, R.C., Daniel, P.T., Bommert, K., Mapara, M.Y., Royer, H.D., Dorken, B., 1996. Induction of the death-promoting gene bax-alpha sensitizes cultured breast-cancer cells to drug-induced apoptosis. Int. J. Cancer 67, 138–141.

Woo, G.H., Katayama, K., Jung, J.Y., Uetsuka, K., Bak, E.J., Nakayama, H., Doi, K., 2003. Hydroxyurea(HU)-induced apoptosis in the mouse fetal tissues. Histol. Histopathol. 18, 387–392.

Woo, G.H., Katayama, K., Bak, E.J., Ueno, M., Yamauchi, H., Uetsuka, K., Nakayama, H., Doi, K., 2004. Effects of prenatal hydroxyurea-treatment on mouse offspring. Exp. Toxicol. Pathol. 56, 1–7.

Yarbro, J.W., 1992. Mechanism of action of hydroxyurea. Semin. Oncol. 19, 1–10.

Yarbro, J.W., Kennedy, B.J., Barnum, C.P., 1965. Hydroxyurea inhibition of DNA synthesis in ascites tumor. Proc. Natl. Acad. Sci. U. S. A. 53, 1033–1035.

Yin, C., Knudson, C.M., Korsmeyer, S.J., Van, D.T., 1997. Bax suppresses tumorigenesis and stimulates apoptosis in vivo. Nature 385, 637–640.

Zambetti, G.P., Bargonetti, J., Walker, K., Prives, C., Levine, A.J., 1992. Wild-type p53 mediates positive regulation of gene expression through a specific DNA sequence element. Genes Dev. 6, 1143–1152.

Available online at www.sciencedirect.com
SCIENCE DIRECT®
Experimental and Toxicologic Pathology 57 (2005) 15–28
EXPERIMENTAL AND TOXICOLOGIC PATHOLOGY
www.elsevier.de/etp

Microarray analysis of T-2 toxin-induced liver, placenta and fetal liver lesions in pregnant rats

Shinya Sehata[a,*], Naoki Kiyosawa[a], Fusako Atsumi[a], Kazumi Ito[a], Takashi Yamoto[a], Munehiro Teranishi[a], Koji Uetsuka[b], Hiroyuki Nakayama[b], Kunio Doi[b]

[a]*Medicinal Safety Research Laboratories, Sankyo Co., Ltd., 717 Horikoshi, Fukuroi-shi, Shizuoka 437-0065, Japan*
[b]*Department of Veterinary Pathology, Graduate School of Agricultural and Life Sciences, The University of Tokyo, 1-1-1 Yayoi, Bunkyo-ku, Tokyo 113-8657, Japan*

Received 4 November 2004; accepted 24 February 2005

Abstract

Pregnant rats on day 13 of gestation were treated orally with 2 mg/kg of T-2 toxin and sacrificed at 1, 3, 6, 9 and 12 h after the treatment (HAT). Histopathologically, the number of apoptotic cells was increased in the liver, placenta and fetal liver (peaked at 6, 12 and 9–12 HAT, respectively). To examine the gene expression profiles, we performed microarray analysis of these tissues at two selected time points based on the results of the TdT-mediated dUTP nick end labeling (TUNEL) staining. Increased expression of oxidative stress- and apoptosis-related genes was detected in the liver of dams, placenta and fetal liver of pregnant rats treated with T-2 toxin at the peak time point of apoptosis. Decreased expression of lipid metabolism- and drug-metabolizing enzyme-related genes was also detected in these tissues. The results suggested that the mitogen-activated protein kinase (MAPK) pathway might be involved in the mechanism of T-2 toxin-induced apoptosis. In addition, increased expression of the *c-jun* gene was consistently observed in these tissues. Our results suggest that the mechanism of T-2 toxin-induced toxicity in pregnant rats is due to oxidative stress followed by the activation of the MAPK pathway, finally inducing apoptosis. The *c-jun* gene may play an important role in T-2 toxin-induced apoptosis.

Keywords: T-2 toxin; Pregnant rats; Liver; Placenta; Fetal liver; Apoptosis; MAPK; Microarray

Introduction

T-2 toxin is a trichothecene mycotoxin produced by various species of *Fusarium* spp. *Fusarium* spp. occurs in cereals including corn, oats, rice and wheat. T-2 toxin has been found to contaminate foods, animal foods and agricultural products, and has been reported in many parts of the world (World Health Organization (WHO), 1990). A single dose or subacute dose of T-2 toxin induces damage in the lymphoid and hematopoietic tissues, resulting in lymphopenia and immunosuppression in

Abbreviations: ERK3, extracellular signal-related kinase 3; GD, gestation day; HAT, hours after treatment; HSP, heat shock protein; MAPK, mitogen-activated protein kinase; MEKK1, mitogen-activated protein kinase kinase 1; RT-PCR, reverse transcriptase-polymerase chain reaction; TUNEL, TdT-mediated dUTP nick end labeling

*Corresponding author. Tel.: +81 538 42 4356, fax: +81 538 42 4350.
E-mail address: sehata@sankyo.co.jp (S. Sehata).

0940-2993/$ - see front matter © 2005 Elsevier GmbH. All rights reserved.
doi:10.1016/j.etp.2005.02.005

many species (Marasas et al., 1969; Hoerr et al., 1981; Hayes and Schiefer, 1982; Pang et al., 1987; Shinozuka et al., 1998). These changes have been shown as being due to apoptosis (Sugamata et al., 1998). Furthermore, T-2 toxin has been shown to affect the central nervous system, although there have been no histopathological changes reported in the adult brain (Martin et al., 1986; WHO, 1990; Wang et al., 1998). It is also reported that pregnant mice treated with T-2 toxin exhibited fetal death and fetotoxicity mainly in the central nervous and skeletal systems in addition to maternal toxicity (Stanford et al., 1975; Rousseaux and Schiefer, 1987; Ishigami et al., 1999, 2001). We showed that apoptosis was observed in the thymus, liver, intestines, placenta, fetal brain and fetal liver at 24 and 48 h after treatment with T-2 toxin in pregnant rats on day 13 of gestation (Sehata et al., 2003). In rats, it is reported that T-2 toxin passes through the placenta and distributes to fetal tissues (Laferge-Frayssinet et al., 1990). Therefore, the apoptotic changes observed in the fetal tissues might be a direct effect of T-2 toxin. Although it is known that T-2 toxin induces lipid peroxidation, protein synthesis inhibition by interaction with ribosomes, and DNA synthesis inhibition (Chang and Mar, 1998; Middlebrook and Leatherman, 1989; Thompson and Wannemacher, 1990), the mechanism of T-2 toxin-induced toxicity is still unknown.

In recent years DNA microarray technologies have been developed. The application of this technology to the field of toxicology has been demonstrated including mycotoxin-induced toxicity. For example, Lühe et al. (2003) reported that ochratoxin A-specific transcriptional changes were detected for genes involved in DNA damage response and apoptosis, response to oxidative stress and inflammatory reactions. We performed microarray analysis of the liver, placenta and fetal liver from pregnant rats 24 h after T-2 toxin treatment (Sehata et al., 2004). According to the results, similar changes in the expression of apoptosis-, lipid metabolism-, drug metabolizing enzyme- and oxidative stress-related genes were detected in these tissues, suggesting that oxidative stress might be involved in the T-2 toxin-induced toxicity. In the above study, we only investigated the changes at 24 or 48 h after the T-2 toxin treatment. However, in general, it is considered that gene expression changes are early event in response to the exposure of chemicals. Therefore, to clarify the detailed mechanism of T-2 toxin-induced changes, earlier time point studies within 24 h after the treatment are necessary.

The purpose of the present study was to examine the detailed morphological changes and gene expression changes within 12 h after T-2 toxin treatment in the liver, placenta and fetal liver obtained from pregnant rats. The protocol of this study was approved by the Animal Care and Use Committee of the Graduate School of Agricultural and Life Sciences, The University of Tokyo.

Materials and methods

Animals

Forty-eight pregnant Wistar:Slc rats on day 11 of gestation (GD11) were obtained from Japan SLC Co., Ltd. (Hamamatsu, Japan). The animals were kept using an isolator caging system (Niki Shoji Co., Ltd., Tokyo, Japan) under controlled conditions (23±2 °C, 55±5% humidity and a 14-h light/10-h dark cycle), and fed commercial pellets (MF; Oriental Yeast Co., Ltd., Tokyo, Japan) and water ad libitum.

Treatments

Based on the results from the dose-finding study (data not shown) and a previously reported study of ours (Sehata et al., 2003), the animals were used on day 13 of gestation (GD13). GD13 is the middle day of organogenesis period in rats, and this period is thought to be sensitive to the chemical-induced toxicity. Therefore, we selected the animals on GD13 for the present study. T-2 toxin (Sigma Chemical Co., MO, USA) was dissolved in corn oil and a dosing volume was adjusted to 2.5 mL/kg. Eighteen animals were treated with a single oral dose of 2 mg/kg T-2 toxin (Sigma Chemical Co., St. Louis, MO, USA), and 3 animals were sacrificed for histopathological examination by exsanguination under ether anesthesia at 1, 3, 6, 9 and 12 h after treatment (HAT), respectively. For microarray analysis, based on the results of the histopathological examination, 9 rats were treated with T-2 toxin in the same way, and 3 rats were sacrificed at 3, 6 and 12 HAT, respectively. T-2 toxin was dissolved in corn oil and the dosing volume was adjusted to 2.5 ml/kg. In addition, a total of 24 animals that were treated with the vehicle alone were used as controls, and 3 animals were sacrificed at 1, 3, 6, 9 and 12 HAT, respectively.

Histopathological examination and immunohistochemical staining

After the animals were sacrificed, a macroscopic examination was performed. Dam's liver, placenta and fetuses from each dam were fixed in 10% neutral-buffered formalin to confirm the changes induced by T-2 toxin. Paraffin sections of 4 μm were stained with hematoxylin and eosin (HE) and subjected to microscopic examination. Cells with fragmented DNA were detected by the TdT-mediated dUTP nick end labeling (TUNEL) method using an apoptosis detection kit

(Apop Tag, Intergen, Purchase, NY, USA). In brief, multiple fragmented DNA-3′-OH ends on the section were labeled with digoxigenin-dUTP in the presence of terminal deoxynucleotidyl transferase (TdT). Peroxidase-conjugated anti-digoxigenin antibody was then reacted with the sections. Apoptotic nuclei were visualized by reacting with peroxidase-diaminobenzidine (DAB). The sections were then counterstained with methyl green. Morphometrical examination was performed in the liver, placenta and fetal telencephalon (3 fetuses/dam) in three randomly selected areas on the section under a light microscope ($\times 400$). The number of positive cells/1000 cells was counted and the mean$\pm$SE of the three measurements was calculated. Statistical analysis was carried out by the Student's *t*-test or Welch's *t*-test after analysis of homogeneity of variance by the *F*-test.

RNA extraction and microarray analysis

Based on the results of the histopathological examination, 9 rats were treated with T-2 toxin, and 3 rats were sacrificed at 3, 6 and 12 HAT, respectively. In addition, 9 rats were treated vehicle, and 3 rats were sacrificed at 3, 6 and 12 HAT, respectively. After the animals were sacrificed, the liver, placenta and fetuses were collected. The fetal liver was collected under stereoscopic microscope. The collected tissues were placed in the tubes and frozen in liquid nitrogen as soon as possible. The frozen tissues were kept under $-80\,^{\circ}C$ until the analysis was performed. Total RNA was extracted from frozen tissues (up to 0.5 g) using the RNeasy Mini Kit (QIAGEN Inc., CA, USA) for the fetal liver or TRIzol reagent (Invitrogen, CA, USA) for the liver and placenta. The RNA from placenta and fetal liver from each dam were pooled to generate a single sample, respectively. The quality of the RNA samples was checked by spectrophotometry according to the Affymetrix protocol. Microarray analysis (total 36 arrays) was performed according to the Affymetrix protocol at the sampling time points (3, 6 and 12 HAT) based on the results of the morphometrical examination. Briefly, cDNA was prepared from 5 μg of total RNA using the SuperScript Choice System for cDNA Synthesis (Invitrogen, CA, USA), with the exception that the primer used for the reverse transcription reaction was a T7-$(dT)_{24}$ primer (primer sequence: 5′-GGC CAG TGA ATT GTA ATA CGA CTC ACT ATA GGG AGG CGG-$(dT)_{24}$-3′, Amersham Biosciences, Tokyo, Japan). Following this, biotin-labeled cRNA was synthesized from the cDNA using the Enzo High Yield RNA Transcription Labeling Kit (Enzo Diagnostics, NY, USA). After 20 μg of biotin-labeled cRNA was fragmented, a hybridization solution was prepared using a GeneChip® Eukaryotic Hybridization Control Kit (Affymetrix Inc., CA, USA) and hybridized to the Affymetrix Rat Genome U34A oligonucleotide array (including 8798 gene probes) at 45 °C for 16 h in a GeneChip® Hybridization Oven 640 (Affymetrix). The chips were washed and stained using the Fluidics Station (Affymetrix) and scanned with a GeneArray® Scanner (Affymetrix). Six chips (each 3 chips for control and T-2, respectively) were used for each time points. We performed the analysis at 3 and 6 HAT in the dam's liver, at 3 and 12 HAT in the placenta and the fetal liver. Therefore, total 36 chips were used.

Data analysis

The quality of the RNA samples used in the microarray analysis was checked by a 5′/3′ ratio of *GAPDH* housekeeping gene probes. The microarray imaging data were analyzed using Microarray Suite Version 5.0 (Affymetrix) and the Spotfire Pro Version 4.2 program (Spotfire Inc., MA, USA). In brief, total array normalization (global normalization after trimming the top 2% and bottom 2% of the data) was performed for all experimental data (Yang et al., 2001). Probes containing at least one *Absence Call* in the data were also removed. We selected genes that gave a mean value changes of greater than +1.5 or less than −1.5. In addition, the mean value of each gene in the treated group was compared with that of the control group by the Student's *t*-test or the Welch's *t*-test after analysis of the homogeneity of variance by the *F*-test. A significance level of $p<0.05$ was considered acceptable.

Real-time reverse transcriptase-polymerase chain reaction (RT-PCR)

GeneChip® results were confirmed by real-time RT-PCR for selected (Table 1). Total RNA (5 μg) from each sample was prepared as the same way described in *RNA extraction and microarray analysis*. RNA was treated with 5 U of DNase I (Takara, Shiga, Japan) in the manufacturer's buffer containing 40 U RNase inhibitor (TOYOBO, Osaka, Japan) in a final volume of 50 μL, and subjected to phenol-chloroform purification. DNase I-treated total RNA of 2 μg was reverse transcribed in a final volume of 20 μL using 200 U of SuperScript II (Invitrogen, CA, USA) in the manufacturer's buffer containing 10 mM DTT, 0.5 mM dNTPs, and 40 U of RNase inhibitor. Real-time PCR was performed using qPCR™ MasterMix Plus (Eurogentec, PA, USA), and the transcription was quantified with a GeneAmp® 5700 Sequence Detection System (Applied Biosystems, CA, USA). For internal control, Rodent GAPDH Control Kit (Applied Biosystems) was used. Statistical analysis for the mean values was carried out by the *F*-test followed by the Student's *t*-test or the Welch's *t*-test.

Table 1. Sequences of oligonucleotide primer/probe used for real-time RT-PCR

Gene (GenBank#)	Primer		TaqMan® probe
c-Jun	Forward	TGCAAAGATGGAAACGACCTT	ACGACGATGCCCTCAACGCCT
(X17163)	Reverse	CCACTCTCGGACTGGAGGAA	
MEKK1	Forward	TCCAGTAACATACACAGGGCAAAG	CATCCCGACCCGTTCCGG
(U48596)	Reverse	CATCCCCTAGTTTGCTTGTGCTA	
Bax-alpha	Forward	CCCCCCGAGAGGTCTTCTT	CGTGTGGCAGCTGACATGTTTGCA
(U59184)	Reverse	CGGCCCCAGTTGAAGTTG	
Heme oxygenase	Forward	TTCTTCTAGCGACAAGTTGATTCTGT	TCCTTGTACCATATCTATACGGCCCT
(J02722)	Reverse	GCTTGTTTCGCTCTATCTCCTCTT	
HSP70	Forward	TGGTGCAGTCGGACATGAA	CACTGGCCCTTCCAGGTGGTGAA
(Z27118)	Reverse	CGGGTAGAACGACCGGTTCT	

Results

Histopathological examination

The T-2 toxin treatment in pregnant rats induced histopathological change, apoptosis, in the liver of dams, placenta and fetal liver. Apoptosis of hepatocytes, cytotrophoblasts in the placenta, and hepatocytes and hematopoietic cells was confirmed by TUNEL staining (Fig. 1). The TUNEL-labeling index was increased at 1 HAT and peaked at 6 HAT in the liver of the dams by the treatment. The labeling index was increased at 1 HAT and was still increased at 12 HAT in the placenta. The labeling index was increased at 1 HAT, and reached a plateau after 9 HAT in the fetal liver (Fig. 2).

Microarray analysis

We selected the time points for microarray analysis based on the histopathological results. In particular, we selected the points at 3 HAT for the three tissues (before the peak time of apoptosis), at 6 HAT for the liver of dams (peak time point of apoptosis), and at 12 HAT for the placenta and fetal liver (peak time point of apoptosis). It is known that T-2 toxin induces apoptosis, lipid peroxidation and suppression of drug-metabolizing enzymes (Chang and Mar, 1998; Guerre et al., 2000; Sehata et al., 2004). Therefore, we focused on cell growth/apoptosis-, stress-, signal transduction-, and lipid- and other metabolism-related genes in the present study.

At 3 HAT in the liver of dams, the expression of 123 genes was increased and that of 140 genes was decreased by T-2 toxin treatment. The expression of the *heat shock protein* (*HSP*) *40-3* and *70* KDa *heat-shock-like protein* genes (stress-related genes) was increased. The expression of apoptosis-related genes such as the *RJG-9* gene for c-jun, *MEKK1* and *tumor necrosis factor receptor* was also increased. Increased expression of inflammation-related genes was detected. In addition, the expression of cell survival- or proliferation-related genes such as *RL/IF-1, p38 MAPK, ERK3* genes was also increased. On the other hand, the expression of lipid metabolism-related genes and drug-metabolizing enzyme genes (*CYP2A2, GST Yc2,* and *rGSTK1-1*) was suppressed by T-2 toxin (Table 2). At 6 HAT in the liver of dams, the peak time point of apoptosis, the expression of 218 genes was increased and that of 253 genes was decreased by T-2 toxin treatment. The expression of stress-related genes (*MnSOD, heme oxygenase* and *HSP86*) was increased. Apoptosis-related genes such as the *Bax-alpha, p21 protein (cip1), TGFB inducible early growth response, ICE-like cystein protease* and *protein kinase (MUK)* genes showed increased expression. In addition, the expression of cell survival- and proliferation-related genes (*NF-kappa B p105 subunit, Bcl2-like 13*) was also increased. On the other hand, the expression of lipid metabolism-related genes such as *17-beta hydroxysteroid dehydrogenase type 2* and *cholesterol 7-alpha-hydroxylas* genes, drug-metabolizing enzyme genes such as *P450d, P450e* and *GST Yc1* genes, and other metabolism-related genes was decreased. The expression of cell growth-related genes such as *cyclin D1* and *cyclin-dependent kinase 4* was also decreased (Table 3).

At 3 HAT in the placenta, the expression of 51 genes was increased and that of 21 genes was decreased by T-2 toxin treatment. The expression of stress-related genes such as the *oxidation resistance* and *NADPH-dependent thioredoxin reductase* genes was increased. The expression of apoptosis-related genes such as the *MEKK1* and *RL/IF-1* genes was increased (Table 4). At 12 HAT, the highest time point of apoptosis, the expression of 137 genes was increased and that of 123 genes was decreased by T-2 toxin treatment. The expression of stress-related genes such as the *HSP70*, and *metallothionein-2* and *-1* genes was increased. The expression of apoptosis-related genes (the *GADD45, p21 (c-Ki-ras),* and *RJG-9* gene for c-jun) was increased. The expression of the cell

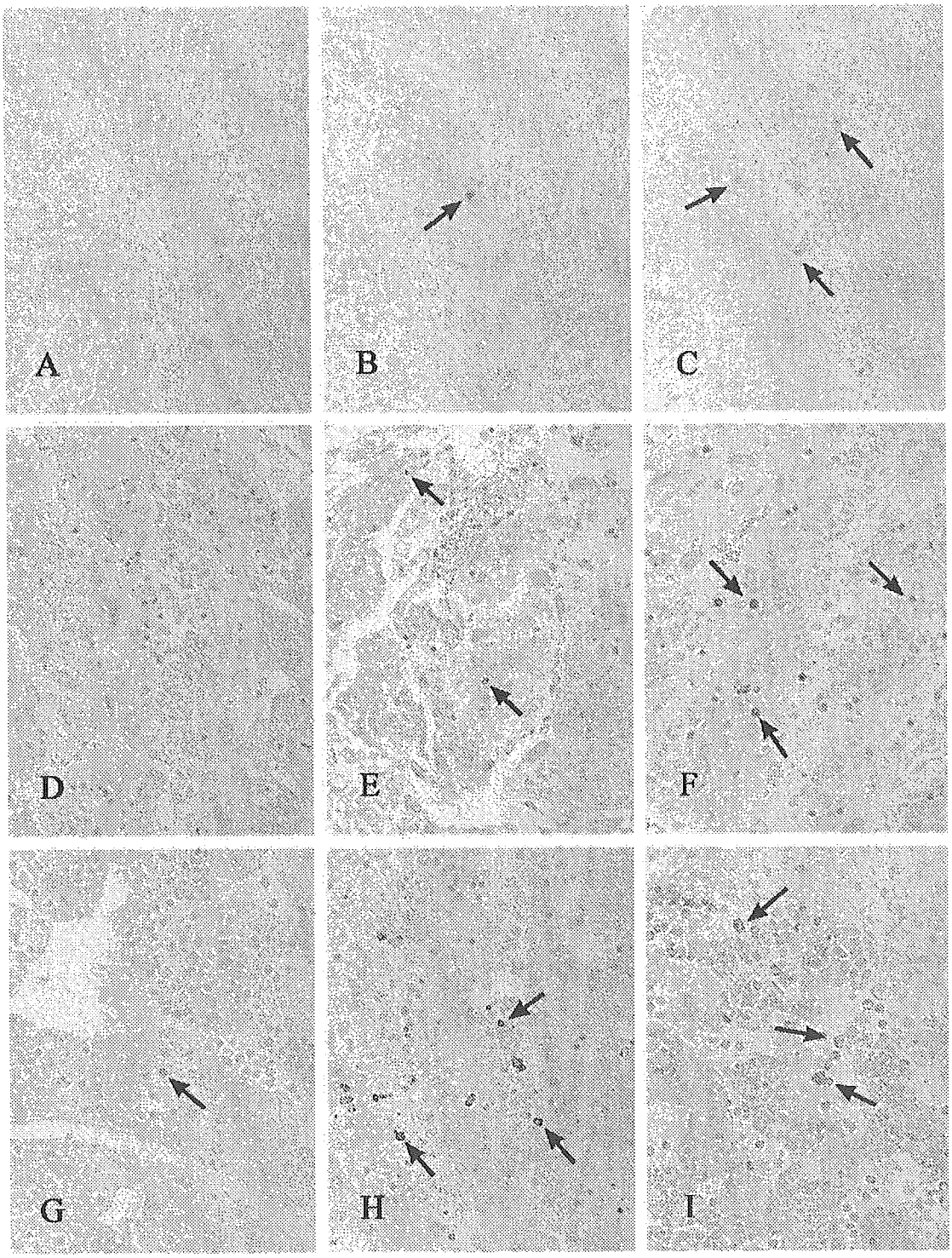

Fig. 1. TUNEL staining in the liver, placenta and fetal liver. The number of TUNEL-positive cells (arrow) was increased by T-2 toxin treatment. (A) A control liver at 12 HAT. (B) A T-2 toxin-treated liver at 3 HAT. (C) A T-2 toxin-treated liver at 12 HAT. (D) A control placenta at 12 HAT. (E) A T-2 toxin-treated placenta at 3 HAT. (F) A T-2 toxin-treated placenta at 12 HAT. (G) A control fetal liver at 3 HAT. (H) A T-2 toxin-treated fetal liver at 3 HAT. (I) A T-2 toxin-treated fetal liver at 12 HAT. TUNEL staining. × 100 (A–C), × 200 (D–I).

survival-related gene (*NF-kappa B p105 subunit*) was also increased. In addition, the expression of inflammation-related genes was also increased. On the other hand, the expression of the lipid metabolism-related genes such as *squalene epoxidase* and *7-dehydrocholesterol reductase* genes, and a drug-metabolizing enzyme

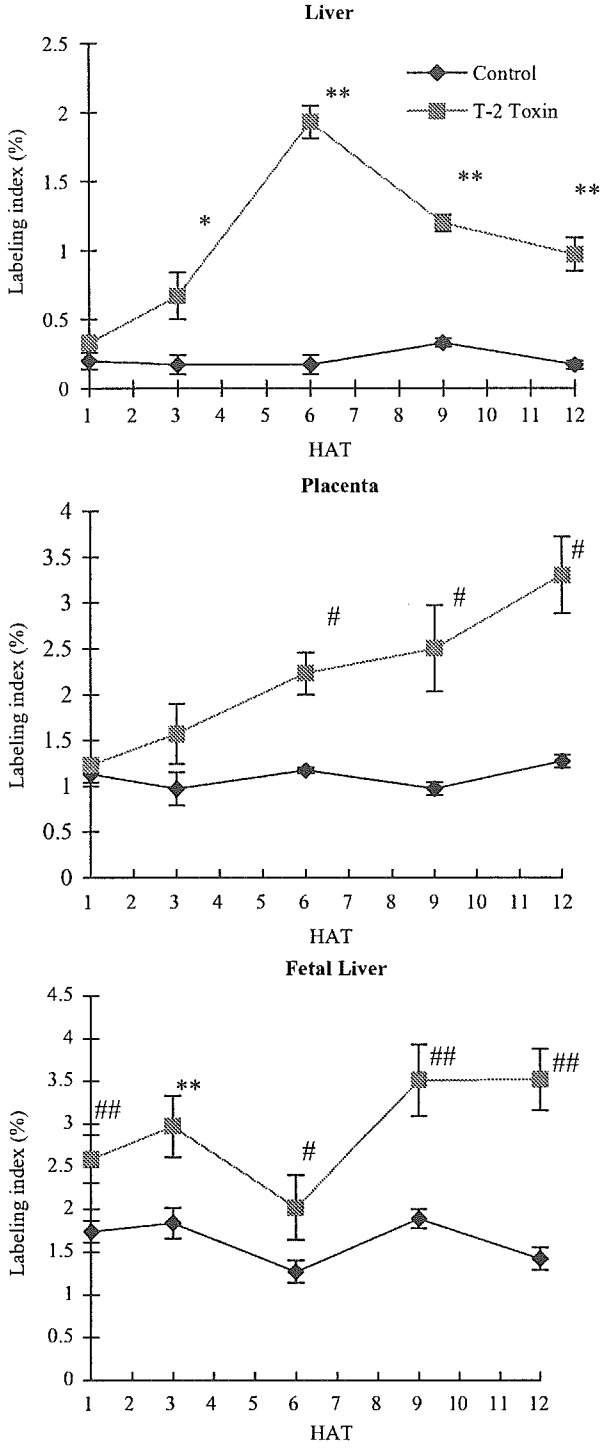

Fig. 2. TUNEL labeling indices in the liver, placenta and fetal liver. The peak time of TUNEL-positive cells was obtained at 6 HAT in the liver, at 12 HAT in the placenta. In the fetal liver, the number of TUNEL-positive cells increased from 1 HAT, and reached a plateau from 9 HAT. Mean±SE. Significantly difference from control: $^{*}p<0.05$, $^{**}p<0.01$ (Student's *t*-test); $^{\#}p<0.05$, $^{\#\#}p<0.01$ (Welch's *t*-test).

gene (*GST Yb*) was decreased. The expression of cell cycle-related genes (*cyclin D1, D3* and *cyclin-dependent kinase 4*) was also decreased (Table 5).

At 3 HAT of the fetal liver, the result obtained from one T-2 toxin-treated animal showed a different gene expression profile from the other two animals (data not shown). The number of fetuses of this animal was 7. The gene expression profile of this animal was different from the other two animals. Although the reason of different expression pattern was unknown, there might be some differences in the severity of the lesion in each obtained fetus of the dam. Therefore, we considered that small number of fetuses might be affected to the obtained data, and that this result was not enough to analysis. Therefore, we excluded the data of the animal from further analysis. However, we show the results of the other two treated-animals as reference data (Table 6). No statistical analysis was performed on this data because of the small number of animals. At 12 HAT, the peak time point of apoptosis, the expression of 86 genes was increased and that of 227 genes was decreased by T-2 toxin treatment. The expression of stress-related genes (*metallothionein-2* and *-1*) was increased. The expression of apoptosis-related genes such as the *Bax, Bax-alpha, Bcl-X-long, GADD45* genes, *RJG-9* genes for c-jun and *c-fos* gene was increased. On the other hand, the expression of lipid metabolism-related genes such as *mitochondrial HMG Co-A synthase* and *17-beta hydroxysteroid dehydrogenase type 2* genes, and drug-metabolizing enzyme genes (*GST Yc2* and *CYP4A3*) was decreased. The expression of cell survival- and apoptosis-related genes (*cyclin D1, p38 MAPK* and *Makp14*) was also decreased (Table 7).

The genes detected in the three tissues are shown in Table 8. The expression of the *RJG-9* gene for c-jun was increased and the expression of the *cyclin D1* gene was decreased in all the tissues. The expression of the *p38 MAPK* gene was increased in the liver of dams and was decreased in the placenta and fetal liver. The expression of the *NF-kappa B* gene and related *RL/IF-1* gene was increased in the liver and placenta of dams. The expression of the *Bax-alpha* gene was increased in the liver of dams and fetal liver.

Real-time RT-PCR

Based on the results of microarray analysis and histopathological examinations (apoptosis), oxidative stress- and apoptosis-related genes were selected to confirm the changes observed in the microarray analysis. Real-time RT-PCR analysis was performed for selected genes and the time points that showed changes in the microarray analysis. The results showed increased expression of the *c-jun, MEKK1, Bax-alpha, HSP70* and *heme oxygenase* genes by T-2 toxin treatment (Fig. 3). Although not all results were completely consistent with those of the microarray analysis,